Computers and Electrical Engineering 000 (2018) 1–17

Contents lists available at ScienceDirect

Computers and Electrical Engineering

journal homepage: www.elsevier.com/locate/compeleceng

Regression model for handover control parameter configuration in LTE-A networks☆

Saraswathi Priyadharshini A*, Bhuvaneswari P.T.V

Department of Electronics Engineering, MIT Campus, Anna University, Chennai, India

ARTICLE INFO

Article history:
Received 29 June 2017
Revised 9 January 2018
Accepted 10 January 2018
Available online xxx

Keywords:
LTE
A3event
Handover control parameters
Inter-site-distance
Regression model

ABSTRACT

In long term evolution - advanced (LTE-A) networks, user assisted and network controlled hard handover (HO) procedure is adopted. In the initial phase of the HO procedure, the transmission of measurement report (MR) is initiated only when the A3 event occurs and persists for the duration of time-to-trigger (TTT). An A3 event is a triggering event which occurs when the signal strength of target evolved NodeB (eNodeB) becomes an offset better than the serving eNodeB. The Hysteresis Margin (HM) and A3Offset (A3Off) are the offset parameters involved in A3 event. Configuration of these parameters plays vital role in HO performance improvement. Most of the configuration methods of these parameters in the literature rely on either optimization rules which is rather complicated for a network of a stochastic nature or on the dynamic characteristics which is not appropriate for the long-term stability of the network. Hence, in this research the cumulative effect of HO control parameters (HCP), such as HM, A3Off and TTT, with respect to inter-site-distance and angle of user equipment movement has been analyzed. From the analysis outcome, a regression based prediction model for HCP configuration has been developed. The presented model outperforms the methods in the literature in terms of serving eNodeB coverage region and HO success region.

1. Introduction

The evolved universal terrestrial radio access network (E-UTRAN), also called long term evolution (LTE), is the access part of the evolved packet system introduced by the third generation partnership project (3GPP) in Release 8 as a flat all-internet protocol (IP)-based architecture [1]. Several technical enhancements are included in LTE to improve the coverage and capacity of the network. It is specified as LTE-advanced (LTE-A) in Release 10 of the 3GPP [2]. The features introduced in LTE-A are carrier aggregation, advanced multi-antenna techniques, relaying and heterogeneous network (HetNet) [3] deployment. The objective of this development is to provide high spectral efficiency, high peak data rates, short round-trip time and flexibility in frequency and bandwidth. The evolved NodeB (eNodeB) is the base station which performs significant and critical functions such as compression and decompression of IP headers, security provision, evolved packet core connectivity, radio resource management functions and mobility management [4]. Tables 1 and 2 present lists of acronyms and symbols used.

In the network, the user equipment (UE) can be in either of the following radio resource control (RRC)-related states, namely, RRC-CONNECTED and RRC-IDLE [5]. Mobility management of UE in the RRC-CONNECTED state is accomplished

☆ Reviews processed and recommended for publication to the Editor-in-Chief by Associate Editor Dr. V. Sai.

* Corresponding author.
E-mail addresses: ajssara@gmail.com (S.P. A), ptvbmit@annauniv.edu (B. P.T.V).

https://doi.org/10.1016/j.compeleceng.2018.01.011
0045-7906/

Table 1
Acronyms and definitions.

Acronyms	Definitions
E-UTRAN	Evolved Universal Terrestrial Radio Access Network
LTE	Long Term Evolution
3GPP	Third Generation Partnership Project
IP	Internet Protocol
LTE-A	LTE-Advanced
HetNet	Heterogeneous Network
eNodeB	Evolved NodeB
UE	User Equipment
RRC	Radio Resource Control
HO	Handover
RAT	Radio Access Technology
MR	Measurement Report
MC	Measurement Configuration
HOF	HO Failure
HCP	HO Control Parameters
ISD	Inter-Site-Distance
RBP	Regression-Based Prediction
RLF	Radio Link Failure
CIO/CSO	Cell-Individual-Offset/ Cell-Specific-Offset
CDR	Call Dropping Ratio
HOR	HO Ratio
CBR	Call Blocking Ratio
RSSI	Received Signal Strength Indicator
CINR	Carrier to Interference plus Noise Ratio
MRO	Mobility Robustness Optimization
HOM	HO Margin
ToS	Time of Stay
HOS	HO Success
RSRP	Reference Signal Received Power
EWPHPO	Enhanced Weighted Performance based HO Parameter Optimization
AHM	Adaptive Hysteresis Margin
UBHO	User Behavior Based Optimization

Table 2
Symbols and definitions.

Symbols	Definitions
Of_n *and* Of_p	Neighbor and primary frequency-specific offset
Oc_n *and* Oc_p	Neighbor and primary cell-specific offset
$SeNB_{Macro}$	Serving macro eNodeB
$TeNB_{Macro}$	Target macro eNodeB
(X_i, Y_i)	Location coordinates of UE
(X_S, Y_S) *and* (X_T, Y_T)	Location coordinates of $SeNB_{Macro}$ and $TeNB_{Macro}$
$\boldsymbol{\beta_T}$	UE distance from the $TeNB_{Macro}$
$\boldsymbol{\beta_{ISD}}$	ISD between $SeNB_{Macro}$ and $TeNB_{Macro}$
$\boldsymbol{\beta_S}$	UE distance from the $SeNB_{Macro}$
$\boldsymbol{\alpha}$	Angle of UE movement
$\boldsymbol{\delta_{A3TP}}$	Distance at which the A3 event occurs
P_T	Received power from the $TeNB_{Macro}$
P_S	Received power from the $SeNB_{Macro}$
$\boldsymbol{\lambda_{TR}}$	Path loss model between T and R
T_P	Transmitter power
$\boldsymbol{\mu_T}$	Transmitter antenna gain
$\boldsymbol{\mu_R}$	Receiver antenna gain
$\boldsymbol{\psi}$	Number of HCP value combinations
$\boldsymbol{\delta_{TTT}}$	Distance covered during TTT
V_{UE}	Velocity of UE
$\boldsymbol{\delta_{A3PD}}$	Distance at which A3 event persists
$\boldsymbol{\delta_{PT}}$	Distance traveled for the duration of HO_{PT}
$\boldsymbol{\delta_{ET}}$	Distance traveled for the duration of HO_{ET}
HO_{PT} *and* HO_{ET}	HO preparation time and HO execution time
P_{ULS}	Uplink received power from $SeNB_{Macro}$
P_{DLS}	Downlink received power from $SeNB_{Macro}$
P_{ULT}	Uplink received power from $TeNB_{Macro}$
R_{HOS}	Region of HOS
$\mathbf{Y}$	Number of HOS groups
G	Configured group
$\boldsymbol{HOS_{LG}}$	Number of locations resulting in HOS for the configured G
NL_{Total}	Total number of locations triggering the HO

Please cite this article as: S.P. A, B. P.T.V, Regression model for handover control parameter configuration in LTE-A networks, Computers and Electrical Engineering (2018), https://doi.org/10.1016/j.compeleceng.2018.01.011

through a UE-assisted and network-controlled hard handover (HO) procedure. The HO procedure is triggered whenever the signal strength of the serving eNodeB is lower than that of the neighbor eNodeB. There are various categories of HO procedure based on the type of radio access technology (RAT) involved, the frequency of operation and the interface availability between two eNodeBs [6]. However, the preparation phase of the HO procedure [7] remains the same irrespective of the HO category.

In this phase, the HO decision is made upon evaluation of the measurement report (MR) from the UE. The MR is triggered by the UE based on the measurement configuration (MC) message [8] received from the serving eNodeB. The MC message contains information relating to when the transmission of MR should be initiated and the mode of sending the MR, i.e., either periodically or based on events defined by 3GPP. Network operators mostly prefer event-based reporting compared to periodic reporting, to avoid wastage of network resources. There are many events defined by the 3GPP standard as event-based reporting criteria. Among the events defined for Intra-RAT HO, event A3 is predominantly used, as it occurs on the basis of relative comparisons rather than absolute comparisons utilizing thresholds.

Apart from the event-based reporting criteria, the 3GPP has defined an additional parameter called the time-to-trigger (TTT) parameter to nullify the effect of dynamic fading characteristics in the wireless environment. The MR will be transmitted to the serving eNodeB only when the A3 event defined in the MC message occurs and persists for the duration of the TTT. The serving eNodeB decides the target eNodeB based on the MR received from the UE. Hence, the triggering time of the MR plays a significant role in the successful completion of the HO procedure. It should not be late or early as this might result in HO failure (HOF). The triggering time of the MR depends on the proper configuration of the parameters involved in the A3event as well as on the value of TTT.

The parameters [8] involved in the A3 event are *Hysteresis Margin (HM), A3Offset (A3Off), cell-specific/individual offsets* (Oc_n and Oc_p) and *frequency-specific offsets* (Of_n and Of_p). The configured values of A3 event parameters and the value of TTT control the success of the HO procedure. Hence, they are called as HO control parameters (HCP). Proper configuration of these HCP becomes mandatory to ensure the success of the HO procedure. In HCP configuration, consideration of factors such as network, UE and environmental characteristics, plays a significant role in the improvement of the HO performance. Among the HCP mentioned above, the cell-specific offset parameters are intended for a deployment scenario with macro and small cells while the frequency-specific offsets are intended for the HO that occurs between eNodeBs with different frequencies of operation. As the presented work is confined to macro-only deployment scenarios with intra-frequency HO (target and serving eNodeB operate on the same frequency), HCP such as Oc_n, Oc_p, Ofn and Of_p are excluded. Hence, the HCP considered in this research are *HM, A3Off* and *TTT* only.

A considerable amount of work has been carried out on HCP configuration to improve the HO performance. There are three methods of HCP configuration adopted in literature: i) optimization methods which search the entire parameter space to arrive at the optimal value, ii) methods which directly compute the optimal HCP on the basis of certain system and user characteristics and iii) hybrid methods which involve both initial configuration and optimization. Compared to other methods, the hybrid approach performs faster and better, as it reduces the search space through initial configuration and then is further optimized for better performance. Other authors have made exhaustive analyses to identify the possible values of HCP based on the system, network, and UE characteristics. The present study involves a hybrid approach. Most of the existing literature considers inter-site-distance (ISD) as a fixed metric, which may not be true in a realistic deployment scenario. Furthermore, the angle made by the UE movement with respect to the line of ISD has a considerable impact on HO performance, as it decides the distance between UE and the corresponding base station.

Therefore, it is evident that a model should be devised for the initial configuration, and that it should be one which utilizes ISD and angle of UE movement to ensure long-term stability of the network. Previous authors have neglected the study of the cumulative effects of the HCP, though the parameters are interrelated and have a significant impact on HO performance. Hence, the objective of this research is to develop a model for the hybrid approach which utilizes ISD and angle of UE movement to configure the HCP, thus improving HO performance. Initially, the dependency of the two metrics ISD and α in the HCP configuration was analyzed. Then, a regression-based prediction (RBP) model for HCP configuration was developed from the outcome of the analysis. The model with higher prediction accuracy was adopted based on the goodness-of-fit metrics. The proposed model was compared with the methods in the literature and was found to outperform them.

The organization of the paper is as follows. Section 2 provides a brief review of related work in the literature. Section 3 explains the adopted system model, the methodology of the proposed analysis and the development of the multiple linearregression-based prediction model. The results and discussion of the research are presented in Section 4. Finally, conclusions and future directions for the work are presented in Section 5.

2. Literature survey

This section discusses the various methods and analyses presented in the literature for HCP configuration to improve HO performance. The optimization method presented in [9] configures the value of both HM and TTT, on the basis of HO performance measures such as radio link failure (RLF) rate, HOF rate, and ping-pong rate. Reconfiguration of HCP is performed by either a zig-zag or a diagonal method of traversal in the parameter search space. The inference from the results is that the diagonal approach converges faster, while better granularity is observed with the zig-zag method. However, degradation in the performance is observed due to the continuous searching procedure involved in the optimization.

Please cite this article as: S.P. A, B. P.T.V, Regression model for handover control parameter configuration in LTE-A networks, Computers and Electrical Engineering (2018), https://doi.org/10.1016/j.compeleceng.2018.01.011

In [10], a sensitivity analysis was performed for the two control parameters cell-individual-offset (CIO) and TTT under different load levels and user velocities. The performance metrics considered in the analysis were call dropping ratio (CDR), HO ratio (HOR) and call blocking ratio (CBR). A fuzzy logic-based optimization technique was designed based on the outcome of the sensitivity analysis. Optimization was performed at three optimization levels, namely, network-wide, cell-wide, and cell-pair-wide levels. The results show achievement of a good trade-off between CDR and HOR for the cell-pair-wide optimization. In [11], optimization criteria were formulated for configuring the values of HM and TTT. The performance metrics considered for optimization were too-late HO, too-early HO, HO to wrong cell, ping-pong HO and unnecessary HO. The HO performance was evaluated in the deployment scenarios with variation in eNodeB transmission power between 20 and 43 dBm. The evaluation results led to the observation that HM and TTT values of 10 dB and 480 ms greatly mitigated the mobility problems, and therefore the presented method improves the HO performance.

The authors in [12] developed two system models for dynamic adoption of the value of HM. The first model utilizes the system metrics called received signal strength indicator (RSSI), while the second is based on carrier to interference plus noise ratio (CINR). The inference from the results is that a similar performance is observed for both methods of HM adaptation. Furthermore, the presented methods reduce the number of redundant handovers without compromising on the throughput, compared to the conventional fixed HM method. In [13], the authors presented a cost-based adaptive HM scheme to minimize the HO failure rate. The cost function is calculated on the basis of system metrics such as the load difference between the target and serving cells and the velocity and service type of UEs. The simulation results obtained led to the inference that the presented cost-based adaptive algorithm outperformed existing methods.

The gradient method-based mobility robustness optimization (MRO) scheme presented in [14] configures the value of the CIO parameter. The derived cost function utilizes performance metrics such as RLF ratio and unnecessary HO ratio. The value of CIO is either increased or decreased in each step, on the basis of the cost function. This leads to improvement in the HO performance irrespective of the user and network characteristics. The UE categorization-based optimization algorithm presented in [15] configures the parameters HO margin (HOM) and TTT. The value of HOM is a combination of HM, A3Off and CIO. The HO performance metrics considered are the number of too-late HO, too-early HO, HO to the wrong cell and ping-pong HO. The control parameters are reconfigured in each step on the basis of the performance metrics. The stability of the algorithm for different velocities and data traffic patterns of UEs was also investigated. The results obtained led to the inference that the presented work outperformed existing methods.

The authors in [16] compute the RLF and ping-pong rates for each TTT and HM configuration with respect to UE speed and deployed configuration. The results show that an RLF rate of less than 2% is achieved when HM is configured to 4 dB for a macro-macro HO scenario, and 0.5 dB for macro-pico and pico-macro HO scenarios. Furthermore, the adaptive TTT value which results in the lowest ping-pong rate was also identified for the selected HM value. In [17], the impact of the HO control parameters namely, TTT, A3Off and cell-specific-offset (CSO) on HO performance in macro-pico deployment was analyzed. The performance metrics considered were State 3 RLF, HOF, time of stay (ToS), ping-pong HO rate and offloading opportunity. A detailed discussion of the dependencies between the HO control parameters with respect to the above mentioned performance metrics is also presented.

The dependency of the HO performance on the ISD considered between macro and femtocells is presented in [18]. Furthermore, the closed-form expressions of the HO performance metrics such as the RLF, HOF and ping-pong rate are derived as functions of ISD and UE speed. Exhaustive simulations have been performed for evaluation of the impact of TTT on the HO performance metrics. The conclusion is that dynamic selection of TTT value based on ISD and UE speed improves the HO performance. In [19], an analysis of the impact of ISD and the type of environment (urban or rural) on successful completion of HO in a macro-macro deployment scenario was undertaken. The control parameters considered were HM, A3Off, and TTT. The simulation results imply that the same combination of control parameters triggers the A3 event too early for smaller ISD and too late for larger ISD. The control parameter combination which results in HOS differs with respect to the type of environment. Hence, it is concluded that during the configuration of control parameters, both the ISD and the type of environment should be considered.

The studies discussed above adopt three different methods of HCP configuration. The studies in [9–11] discuss optimization methods which search for the optimal HCP in the entire parameter space on the basis of HO performance. Expert knowledge from the perspective of the network's operation is required for early confinement with the optimal HCP setting. It is also highly unlikely that rules can be formulated considering the wider system characteristics. The authors in [12,13] developed the models which directly compute the optimal HCP based on certain system and user characteristics. In these methods, dynamic characteristics such as the load and the velocity and service type of the UE, cause large fluctuations in the HO performance. The methods discussed in [14,15] form a hybrid approach which involves two phases. In the initial phase, the system characteristics are utilized for the initial configuration of HCP, and, in the second phase, the configured HCP is optimized on the basis of various performance metrics. The hybrid approach has the advantage of reducing the search space, but also has the drawback of depending on the dynamic characteristics of the system.

The literature in [16–19] investigates the sensitivity of the HO performance to control parameters with respect to the various system, network and UE characteristics, in order to provide meaningful insights into the impact of the characteristics on HO performance. It is evident from the literature that a hybrid approach which utilizes certain HO performance dependent characteristics in the initial configuration must be devised for ensuring the long-term stability of the network. As mentioned in an earlier section, there has previously been less focus on ISD and angle of UE movement. Also, despite each HCP having its own significance in network performance improvement, wide variations are observed with respect to

Please cite this article as: S.P. A, B. P.T.V, Regression model for handover control parameter configuration in LTE-A networks, Computers and Electrical Engineering (2018), https://doi.org/10.1016/j.compeleceng.2018.01.011

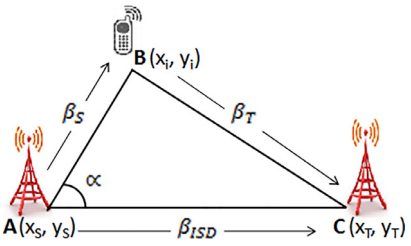

Fig. 1. System model.

HCP consideration among the various studies. Therefore, in this research, a RBP model has been developed, utilizing the dependency of ISD and angle of UE movement on HO performance for HCP configuration.

3. Proposed methodology

This section discusses in detail the system model considered and the methodology proposed for the study of the impact of system characteristics such as ISD and angle of UE movement on HCP configuration to improve the HO performance.

3.1. System model

The system model considered in the proposed methodology is presented in Fig. 1. Let $SeNB_{Macro}$ be the serving macro eNodeB located at A with coordinates (X_S, Y_S), $TeNB_{Macro}$ be the target macro eNodeB located at C with coordinates (X_T, Y_T), and let the UE be located at B with coordinates (X_i, Y_i). Let β_{ISD} be the ISD between $SeNB_{Macro}$ and $TeNB_{Macro}$. The UE is assumed to move in a straight line making an angle of α with respect to the line of β_{ISD}. At any instant, the UE is considered to be at distance β_S from the $SeNB_{Macro}$ and β_T from the $TeNB_{Macro}$.

3.2. Proposed analysis

In order to model the dependency of β_{ISD} and α on the combinations of HCP values resulting in HO Success (HOS), an analysis has been performed as illustrated in Fig. 2. The HCP considered are HM, A3Off and TTT. Various macro-macro HO scenarios with different values of β_{ISD} and α are simulated. Each scenario is configured with different combinations of HCP values. For each scenario, the method identifies whether or not the configured combinations of HCP values result in HOS. The success of the HO procedure is determined on the basis of evaluation of the following three conditions: i) A3 event occurrence, ii) A3 event persistence and iii) HO completion. A brief explanation of these conditions is presented in the following sections. Initially, the occurrence and persistence of the A3 event for the configured combination of HCP values, is verified. Upon persistence of the A3 event, the transmission of MR to the $SeNB_{Macro}$ is triggered otherwise the control parameters are reconfigured with the next combination of HCP values. Let ψ be the number of combinations of HCP values considered in this study. For each scenario, ψ combinations are configured and verified for its success.

The analysis is repeated for all the simulation scenarios considered. The HCP value combinations that result in HOS are identified for each scenario. The combinations of HCP values which result in failure are categorized as the HOF group.

3.2.1. Evaluation of A3 event occurrence

Let δ_{A3TP} be the distance at which the A3 event occurs when the UE moves from $SeNB_{Macro}$ to $TeNB_{Macro}$. The occurrence of the A3 event is identified using Eq. (1).

$$\delta_{\text{A3TP}} = P_T - HM > P_S + A3Off \tag{1}$$

where P_T represents the power received from the $TeNB_{Macro}$ at β_T and P_S is the power received from the $SeNB_{Macro}$ at β_S. Both are measured in dBm and are computed using Eq. (2).

$$P_S = P_T = T_P - \lambda_{TR} + \mu_T + \mu_R \tag{2}$$

where T_P indicates the transmitter power, λ_{TR} is the path loss model between transmitter (T) and receiver (R), and μ_T and μ_R denote the antenna gains of T and R. The occurrence of the A3 event is verified for all the combinations of HCP values at consecutive coordinates (X_i, Y_i) during the movement of UE with respect to the $SeNB_{Macro}$. Then, the combinations of HCP values that result in the occurrence of the A3 event at the same D_{A3TP}, are grouped into one category.

3.2.2. Evaluation of A3 event persistence and transmission of MR

Once the A3 event occurs, the persistence of the A3 event is verified after TTT duration, in order to avoid frequent and unnecessary HO. A lower value of TTT is considered for maximum V_{UE} [16]. The number of combinations of HCP values

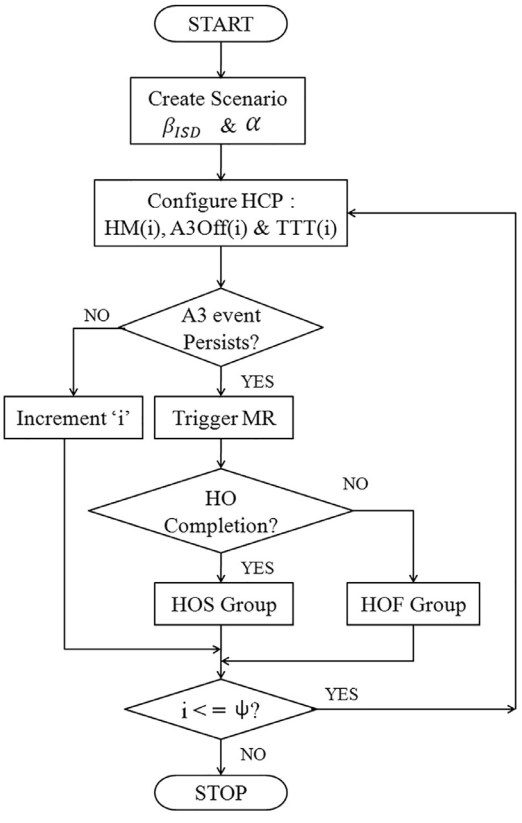

Fig. 2. Proposed analysis.

(ψ) remains the same, as only one value of TTT is considered. Let δ_{TTT} be the distance covered by the UE during the TTT duration. This is computed using Eq. (3).

$$\delta_{TTT} = \frac{V_{UE}}{TTT} \tag{3}$$

The transmission of MR is initiated towards the $SeNB_{Macro}$ by the UE if the A3 event persists over the distance δ_{TTT}. Let δ_{A3PD} be the distance at which the A3 event persists. This depends on both δ_{A3TP} and δ_{TTT}, as shown in Eq. (4).

$$\delta_{\mathrm{A3PD}} = \delta_{\mathrm{A3TP}} + \delta_{\mathrm{TTT}} \tag{4}$$

3.2.3. Evaluation of HO procedure completion

Let δ_{PT} and δ_{ET} denote the distance traveled by the UE during the HO preparation time ($\mathrm{HO_{PT}}$) and HO execution time ($\mathrm{HO_{ET}}$). Let $\mathrm{P_{ULS}}$ be the uplink received power with respect to $SeNB_{Macro}$ at the distance δ_{A3PD}, let $\mathrm{P_{DLS}}$ indicate the downlink received power with respect to $SeNB_{Macro}$ at the distance ($\delta_{\mathrm{A3PD}} + \delta_{\mathrm{PT}}$) and let $\mathrm{P_{ULT}}$ be the uplink received power with respect to $TeNB_{Macro}$ at the distance ($\delta_{\mathrm{A3PD}} + \delta_{\mathrm{PT}} + \delta_{\mathrm{ET}}$). Let RSRP_{min} be the minimum reference signal received power (RSRP) required by the UE to obtain service from the corresponding eNodeB. Let RSRP_{RLF} represent the RSRP value which results in RLF. Upon receiving the MR, the $SeNB_{Macro}$ triggers the HO to the respective $TeNB_{Macro}$.

The HO procedure is completed successfully only when the following three conditions are satisfied: i) successful reception of UE generated MR by $SeNB_{Macro}$ at δ_{A3PD}, which is possible when $\mathrm{P_{ULS}}$ is greater than or equal to RSRP_{min} as mentioned in Eq. (5), ii) $\mathrm{P_{DLS}}$ is greater than RSRP_{RLF} for the successful reception of the HO command message by UE after $\mathrm{HO_{PT}}$ as in Eq. (6) and iii) as presented in Eq. (7), $\mathrm{P_{ULT}}$ is greater than or equal to RSRP_{min} so that the radio link persists with $TeNB_{Macro}$ after the duration of $\mathrm{HO_{ET}}$.

$$\mathrm{P_{ULS}}(\delta_{\mathrm{A3PD}}) \geq \mathrm{RSRP}_{min} \tag{5}$$

$$\mathrm{P_{DLS}}(\delta_{\mathrm{A3PD}} + \delta_{\mathrm{PT}}) > \mathrm{RSRP}_{RLF} \tag{6}$$

$$\mathrm{P_{ULT}}(\delta_{\mathrm{A3PD}} + \delta_{\mathrm{PT}} + \delta_{\mathrm{ET}}) \geq \mathrm{RSRP}_{min} \tag{7}$$

Please cite this article as: S.P. A, B. P.T.V, Regression model for handover control parameter configuration in LTE-A networks, Computers and Electrical Engineering (2018), https://doi.org/10.1016/j.compeleceng.2018.01.011

This procedure is extended to all β_{ISD} and α considered in the analysis for the study of the impact of HCP value combinations on HO performance. In the presented research, the performance of the HO procedure is analyzed using metrics such as *number of HOS groups* (γ) and *region of HOS* (R_{HOS}). The metric γ is defined as the number of HCP groups which result in HO success, while the metric R_{HOS} defines the percentage of the total region within which the HO initiated by the particular HCP group results in success. The possibility percentage of HOS is given by R_{HOS}. This metric is presented in Eq. (8).

$$R_{HOS}(\%) = \frac{HOS_G}{NL_{Total}} * 100 \tag{8}$$

where HOS_G represents the number of locations which result in HO success for the configured group G, $G = 1$ *to* γ, and NL_{Total} represents the total number of locations considered for triggering the HO.

3.3. Regression model development

The outcome of the above analysis leads to the inference that HO performance exhibits a high dependency on system characteristics, such as β_{ISD} and α. Hence, they are used as predictors for the development of RBP model. Both are considered, as two independent variables of the RBP model, while γ, the number of HOS groups for a particular simulation scenario, is taken as the dependent variable. The prediction accuracy of the model is dependent on the degree of the independent variables. The higher the degree of the variable, better the prediction accuracy. Let us consider the degrees of the independent variables β_{ISD} and α to be 'p' and 'q' respectively. The RBP model with degree $p = q = 1$ takes the form shown below.

$$\gamma = \varphi_1 + \varphi_2 \beta_{ISD} + \varphi_3 \propto \tag{9}$$

where φ_1, φ_2 and φ_3 are the unknown coefficients. Eq. 10 represents the matrix form of above linear model for 'n' number of inputs. Let 'm' represents the number of unknown coefficients which depend on the degree of the independent variables and 'n' represents the number of simulation scenarios.

$$\gamma^{pq}_{n\times 1} = P^{pq}_{n\times m} * \varphi^{pq}_{m\times 1} \tag{10}$$

where $\gamma^{pq}_{n\times 1}$ is the $(n \times 1)$ matrix representing number of HOS groups identified for 'n' simulation scenarios, φ^{pq}_{mx1} is the $(m \times 1)$ matrix indicating the unknown coefficients and $P^{pq}_{n\times m}$ is the design matrix for the regression model. Eq. (11) presents the expanded forms of each of the metrics in Eq. (10) for $p = 1$ & $q = 1$.

$$\gamma^{11}_{nx1} = \begin{bmatrix} \gamma_1 \\ \vdots \\ \vdots \\ \gamma_n \end{bmatrix}, \varphi^{11}_{mx1} = \begin{bmatrix} \varphi_1 \\ \vdots \\ \vdots \\ \varphi_m \end{bmatrix}, P^{11}_{nxm} = \begin{bmatrix} 1 & \beta_{ISD(1)} & \propto_1 \\ \vdots & \vdots & \vdots \\ \vdots & \vdots & \vdots \\ 1 & \beta_{ISD(n)} & \propto_n \end{bmatrix} \tag{11}$$

To develop the RBP model, the values of the unknown coefficients are computed using Eq. (12) for any degree of the independent variables.

$$\varphi^{pq}_{m\times 1} = ((P^{pq}_{n\times m})^T * P^{pq}_{n\times m})^{-1} * ((P^{pq}_{n\times m})^T * \gamma^{p}_{n\times 1} q) \tag{12}$$

The sensitivity of the developed model is verified with the goodness of fit metrics such as sum of squares due to error (SSE), R-square, adjusted-R-square and root mean squared error (RMSE) [20].

4. Results

This section discusses the results of the analysis and the developed RBP model. The simulations are performed using MATLAB R2014a and the simulation parameters are given in Table 3. The values configured for the simulation parameters follow 3GPP specifications. In this section, the impact of considering all the A3 event parameters is presented, followed by the sensitivity analysis with respect to distance-related metrics such as β_{ISD} and α. Furthermore, a dependency analysis of β_{ISD} and α on the region of HOS for each of the configured groups, is performed. On the basis of the outcome of the analysis, an RBP model is developed to configure the HCP. The RBP model with the highest prediction accuracy is identified based on goodness-of-fit metrics. Finally, the results are compared with methods in the literature.

In this study, the values of HM, A3Off and TTT in the range specified by 3GPP have been considered in the analysis. The HM values in intervals of 5 dB have been assumed, and these values are {0, 5, 10, 15 dB}. Similarly, A3Off takes seven values {−15, −10, −5, 0, 5, 10, 15 dB}. The analysis has been made for a high mobility ($V_{UE} = 110$ km/h) UE, taking into account the fact that the combination of HCP values which results in HOS for high mobility UE will be highly suitable for low mobility UE also. Hence, a TTT value of 40 ms is assumed, as the analysis considers maximum V_{UE} [16].

From the above specification for the macro-macro scenario, 28 combinations (=4(HM values)*7(A3Off values)*1(TTT value)) are formulated to analyze the sensitivity of these parameters on HO performance. Furthermore, the simulation scenarios based on the system model presented in Fig. 1. have been used. This involves scenarios with different values of β_{ISD},

Please cite this article as: S.P. A, B. P.T.V, Regression model for handover control parameter configuration in LTE-A networks, Computers and Electrical Engineering (2018), https://doi.org/10.1016/j.compeleceng.2018.01.011

Table 3
Simulation parameters.

Parameter	Configured value
Transmitter Power (T_P)	Macro eNodeB: 46 dBm
Macro Propagation Model (λ_{TR})	$128.31 + 37.6 \log_{10}$R, 'R' in Km [22]
Time-To-Trigger	40 ms [16]
UE Transmit Power	30 dBm
HO Preparation Time (HO_{PT})	50 ms [21]
HO Execution Time (HO_{ET})	40 ms [21]
Radio Link Failure ($RSRP_{RLF}$)	−130 dBm
Velocity of UE (V_{UE})	Urban: Upto 110 Km/h
Minimum required RSRP ($RSRP_{min}$)	−110 dBm (to camp on respective eNodeB)
Antenna gain after cable loss (μ_T)	Macro eNodeB: 15 dBi
eNodeB antenna height (Ht_{eNB})	15 m [22]
Carrier Frequency (F_c)	2 GHz
Antenna Pattern	Omnidirectional
HO Control Parameters	HM: 0–15 dB & A3Off: −15 to 15 dB [8]

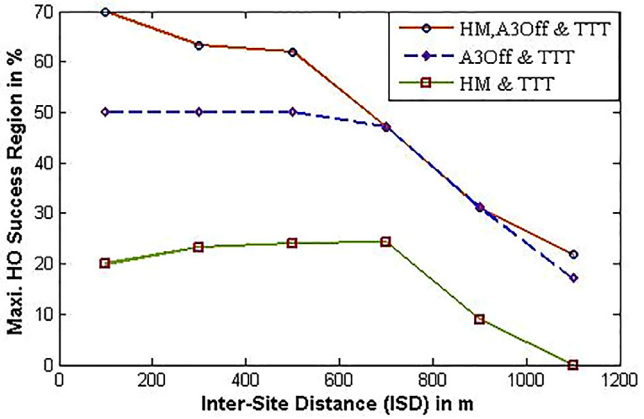

Fig. 3. Impact of control parameters.

such as 100 m, 300 m, 500 m, 700 m, 900 m and 1100 m and of α, such as 10°, 30°, 50°, 70° and 90°. It results in a set of 30 (= 6(β_{ISD} values)*5(α values)) simulation scenarios. All 28 combinations of HCP values are configured for each simulation scenario to identify the combination which results in successful HO completion. Hence, 840 (= 28*30) simulation runs were made to study the sensitivity of the parameters with respect to the scenario.

4.1. Impact of control parameters

In order to justify the need for studying the cumulative effect of HCP, the impact on the maximum HO success region of three different HCP combination cases has been considered. These are: case 1, involving a combination of HM, A3Off and TTT, case 2, representing the combination of A3Off and TTT and case 3, representing the combination of HM and TTT. In all the cases, TTT is adopted mandatorily as it is configured to nullify the negative effects of fading in a wireless environment. Fig. 3 shows the impact of considering different combinations of HCP on the maximum HO success region.

The results show that consideration of all the HCP improves the HO success region, compared to the other cases. For $\beta_{ISD} = 100$ m, case 1 achieves 70% of the HOS region, which is 40% higher than for case 2 and 100% higher than for case 3. This is because a positive value of A3Off triggers a late HO, as it makes the serving eNodeB more favorable for service provision, and postpones the HO. This condition is reversed for a negative value of A3Off. Similarly, the positive value of HM further delays the HO compared to the positive value of A3Off, as it makes the target eNodeB less favorable for HO. It can also be observed that as β_{ISD} increases, the region of HOS decreases, as the overlapping region decreases with an increase in β_{ISD}. This analysis clearly indicates that studying the combined impact of HCP plays a vital role in improving the possibility of HOS and is dependent on β_{ISD}.

4.2. Sensitivity analysis

The sensitivity analysis is performed at two different levels. Level 1 analyzes the influence of β_{ISD} on R_{HOS} and level 2 analyzes the influence of α on R_{HOS}. Fig. 4a–f represents the influence of β_{ISD} on R_{HOS} when α is assumed to be 45°.

Please cite this article as: S.P. A, B. P.T.V, Regression model for handover control parameter configuration in LTE-A networks, Computers and Electrical Engineering (2018), https://doi.org/10.1016/j.compeleceng.2018.01.011

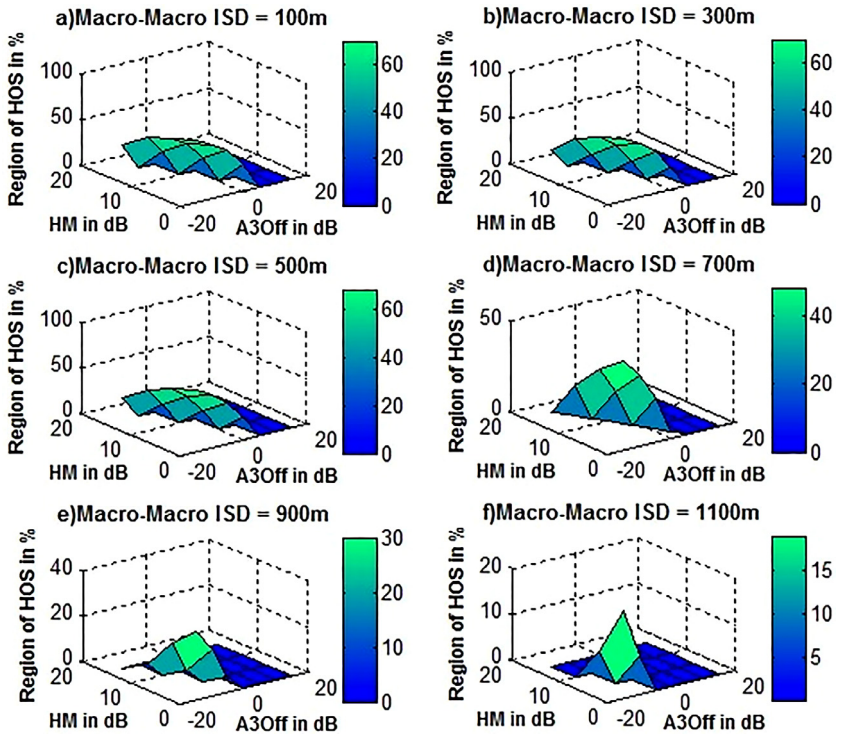

Fig. 4. Sensitivity analysis of β_{ISD}.

It is observed that up to 500 m of β_{ISD}, the maximum HOS region achieved is 70% when HCP is configured with G_1. However, when β_{ISD} increases beyond 500 m, it can be observed that the region of HOS reduces. This is because the overlapping region between the serving and target eNodeB reduces with an increase in β_{ISD}. Thus, the success of HO is highly sensitive to β_{ISD}. The sensitivity analysis helps to identify β_{ISD} as a potential prediction metric for development of a model for optimal HCP configuration. The analysis is further extended to study the impact of α on R_{HOS}.

Fig. 5a–e illustrates the influence of α on R_{HOS} when β_{ISD} is assumed to be 500 m. When α is 10°, the maximum region of HOS achieved is 66.14%. However as α increases, the region reduces, because the distance between UE and the target eNodeB increases. Hence the maximum angle for which the HOS can be achieved with the considered target eNodeB is 45°. Beyond this angle, HO can be achieved with the other adjacent target eNodeB.

Thus, the success of the HO procedure is sensitive to variations in α. In summary, the results reveal that the combinations of HCP values which trigger the HO early result in an increased HOS region. For these, the HM values fall in the range 0 to 10 dB, while A3Off falls in the range 0 to −15 dB. Therefore, HO which is triggered early presents a higher probability of HOS with a smaller serving eNodeB coverage region, and vice-versa. Delayed triggering occurs when A3Off falls in the range 0 to 15 dB, leading to a high probability of HOF. Thus, the dependency of the HO performance on β_{ISD} and α on HO performance is presented.

4.3. Formulation of HO control parameter combination groups

As mentioned earlier, the 28 combinations of HCP values were configured to 30 simulation scenario sets, and the success of the HO procedure was verified for each of the combinations. During the simulations, it was observed that the trigger point for HO was same for certain combinations of HCP values, and these are grouped together in Table 4. There are ten such groups, from G1 to G10. Further analysis and the model development are discussed in terms of groups instead of individual combinations of HCP values. For investigating the formulated groups, a pictorial representation of the groups and their HO trigger points was produced, as shown in Fig. 6. It can be seen that groups G1–G3 trigger the HO in the early HO region ($\mathrm{Early_{HOR}}$) while G4 triggers exactly at the intersection point. The groups from G5 to G10 trigger the HO in the late HO region ($\mathrm{Late_{HOR}}$).

The sum of HM and A3Off, i.e., HOM, is negative for $\mathrm{Early_{HOR}}$ and positive for $\mathrm{Late_{HOR}}$. The HO is triggered exactly in the middle when their sum is zero. Consideration of both HM and A3Off results in HOM values from −15 dB to 30 dB, providing the possibility of triggering HO over a wider region.

The early trigger groups, such as G1, G2 and G3, reduce the time of association with the serving cell, as the HO is triggered well before the boundary, while the case is reversed for the late trigger groups from G5 to G10.

Please cite this article as: S.P. A, B. P.T.V, Regression model for handover control parameter configuration in LTE-A networks, Computers and Electrical Engineering (2018), https://doi.org/10.1016/j.compeleceng.2018.01.011

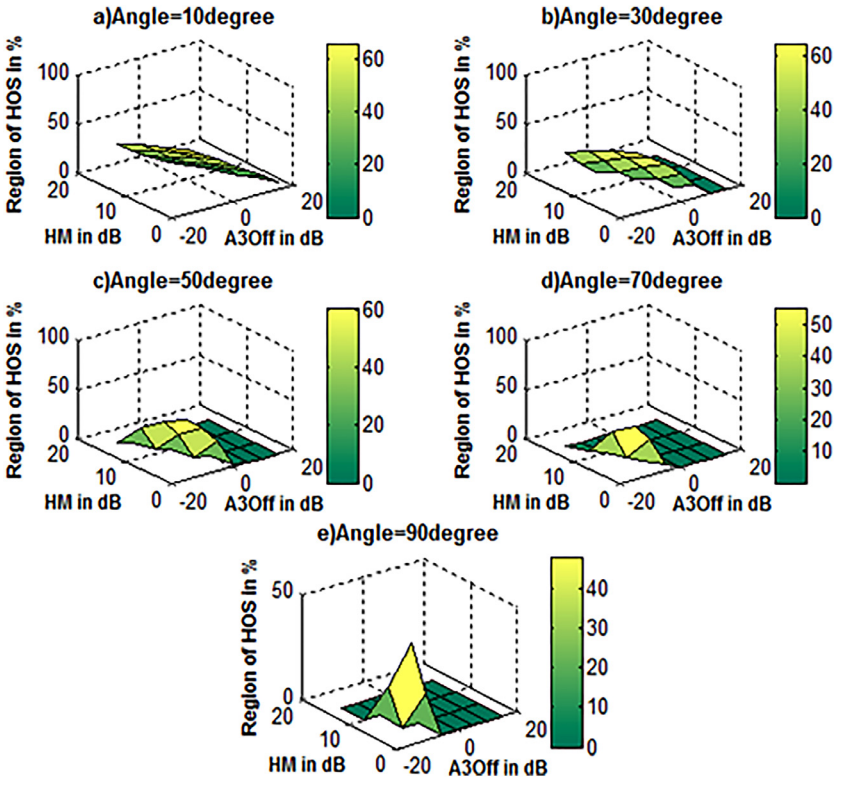

Fig. 5. Sensitivity analysis of α.

Table 4
Groups with the same D_{A3TP}.

Group	(HM, A3Off) in dB
G1	(0, −15)
G2	(5, −15) (0, −10)
G3	(10, −15) (5, −10) (0, −5)
G4	(15, −15) (10, −10) (5, −5) (0, 0)
G5	(15, −10) (10, −5) (5, 0) (0, 5)
G6	(15, −5) (10, 0) (5, 5) (0, 10)
G7	(15, 0) (0, 15) (10, 5) (5, 10)
G8	(5, 15) (10, 10) (15, 5)
G9	(15, 10) (10, 15)
G10	(15, 15)

4.4. Impact of ISD and angle of UE movement on HO success

Fig. 7 presents the impact analysis of both β_{ISD} and α in terms of the number of groups resulting in HOS (γ). As the combination of HCP values in each group initiates the HO at the same point, anyone of the combinations from each group was configured. A value of γ equal to two in the figure represents groups G1 and G2, while groups G1, G2 and G3 are represented by γ equal to three, and so on. It is observed that the same value of γ occurs for β_{ISD} of upto 500 m, which is the optimal ISD as given by 3GPP specifications. When β_{ISD} increases beyond 500 m, the value of γ begins to decrease. The reason for this is that the overlapping region between the serving and target eNodeB decreases with an increase in β_{ISD}, leading to a higher probability of RLF occurrence before the successful completion of the HO procedure. A significant impact of α on γ was observed irrespective of the optimal β_{ISD}. This is because, as α increases, the distance between the target eNodeB and the UE increases for the same distance between UE and the serving eNodeB. Fig. 7 shows that γ decreases with an increase in β_{ISD} and α. The inference is that the HO should be initiated earlier with increases in both β_{ISD} and α, and vice-versa.

In addition, the configuration of the same HCP, irrespective of β_{ISD} and α, degrades the overall HO performance. This suggests the need for dynamic configuration of HCP based on β_{ISD} and α, rather than fixed configuration of HCP.

Please cite this article as: S.P. A, B. P.T.V, Regression model for handover control parameter configuration in LTE-A networks, Computers and Electrical Engineering (2018), https://doi.org/10.1016/j.compeleceng.2018.01.011

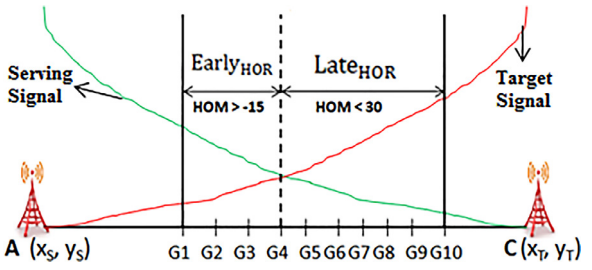

Fig. 6. Early and late HO regions with respect to the formulated groups.

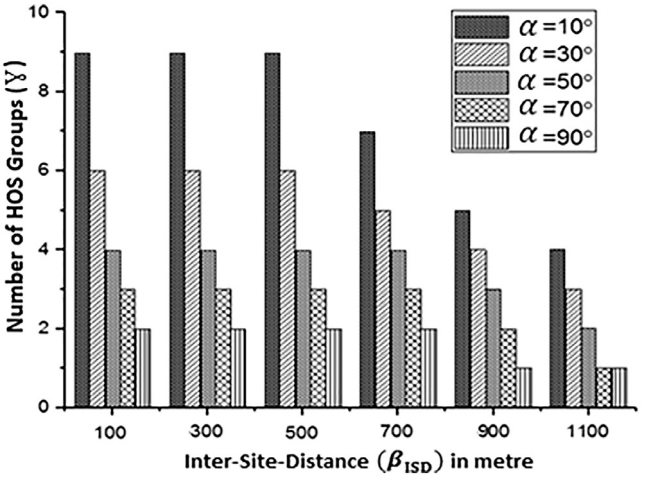

Fig. 7. Impact of ISD and angle on UE movement analysis.

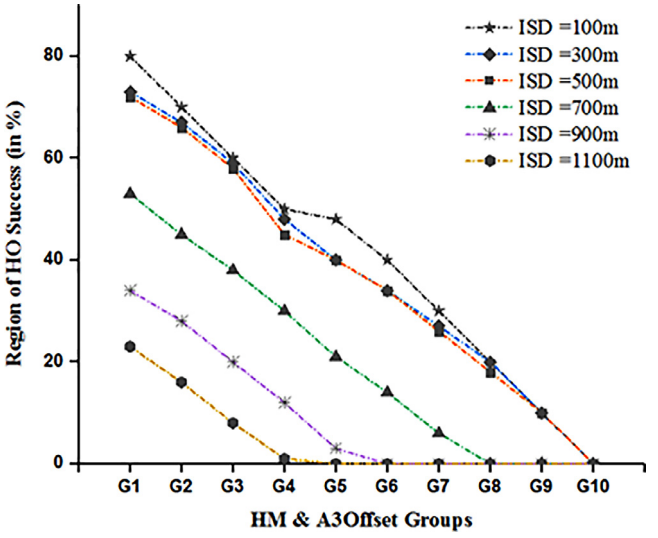

Fig. 8. Impact of β_{ISD} on R_{HOS} for the configured groups with $\alpha = 10°$.

4.5. Analysis on region of HOS with respect to groups

The analysis has been extended to visualize the R_{HOS} for each HOS group configured. Utilizing the symmetrical property, the analysis was performed for $\alpha = 10°$, 30° and 50°. Figs. 8–10 represent the analysis of R_{HOS} for each configured group, and β_{ISD} with fixed α values of 10°, 30° and 50°. Fig. 8 shows that when β_{ISD} is varied from 100 m to 500 m, the R_{HOS} (%) is somewhat similar but varies between 80% and 10% (G1 to G9) with respect to the configured HCP groups. A decrease in the HOS region is observed: i) from 55% to 5% (G1 to G7) for a β_{ISD} of 700 m, ii) from 35% - 4% (G1 to G5) for a β_{ISD} of

Please cite this article as: S.P. A, B. P.T.V, Regression model for handover control parameter configuration in LTE-A networks, Computers and Electrical Engineering (2018), https://doi.org/10.1016/j.compeleceng.2018.01.011

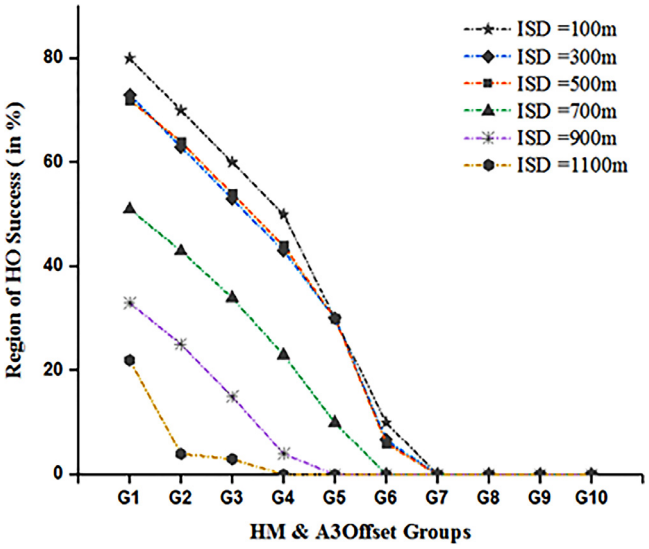

Fig. 9. Impact of β_{ISD} on R_{HOS} for the configured groups with $\alpha = 30°$.

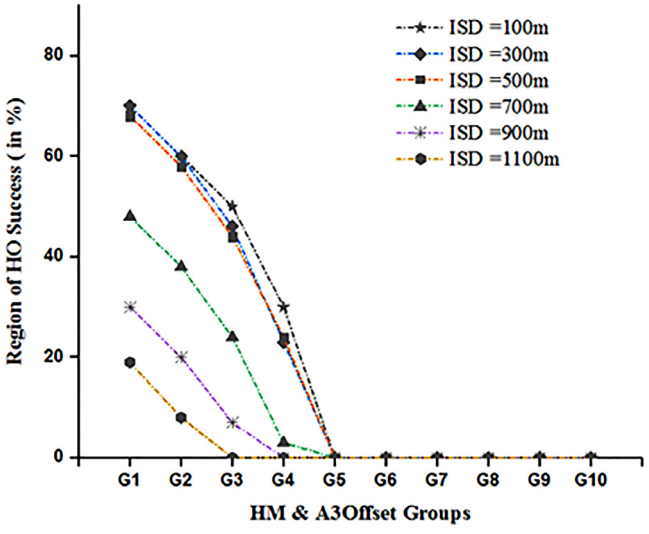

Fig. 10. Impact of β_{ISD} on R_{HOS} for the configured groups with $\alpha = 50°$.

900 m and iii) from 23% to 2% (G1 to G4) for a β_{ISD} of 1100 m. A similar analysis is presented in Figs. 9 and 10 for $\alpha = 30°$ and 50°. Fig. 9 shows that for $\alpha = 30°$ the R_{HOS} is similar for β_{ISD} between 100 m and 500 m, but varies from 80% - 7% (G1 to G6) with respect to the HCP groups. As β_{ISD} increases, the R_{HOS} decreases further: i) from 52% to 10% (G1 to G5) for a β_{ISD} of 700 m, ii) from 35% to 4% (G1 to G4) for a β_{ISD} of 900 m and iii) from 21% to 2% (G1 to G3) for a β_{ISD} of 1100 m.

From Fig.10, for $\alpha = 50°$, it can be observed that the R_{HOS} is almost similar for β_{ISD} of 100 m to 500 m, but with variation from 70% to 23% (G1 to G4) with respect to the configured HCP groups. As β_{ISD} increases, the R_{HOS} decreases further: i) from 50% to 2% (G1 to G4) for a β_{ISD} of 700 m, ii) from 30% to 6% (G1 to G3) for a β_{ISD} of 900 m and iii) from 20% to 8% (G1 to G2) for a β_{ISD} of 1100 m. The above analysis shows the same HCP combination resulting in different R_{HOS} with respect to α and β_{ISD}. This is because the increase in β_{ISD} decreases the overlapping region and the triggering time of HO. Also, early triggering results in a larger R_{HOS}, while late triggering decreases the R_{HOS}.

$$R_{HOS} = \frac{1}{\Delta(\alpha, \beta_{ISD})} \tag{13}$$

Eq. (13) illustrates the relationship established between R_{HOS}, β_{ISD} and α via the above analysis. It is found that R_{HOS} is inversely proportional to both α and β_{ISD}. Based on these conclusions, the dependency of β_{ISD} and α on HCP configuration has been modeled as regression based prediction model and is presented in the following section.

Please cite this article as: S.P. A, B. P.T.V, Regression model for handover control parameter configuration in LTE-A networks, Computers and Electrical Engineering (2018), https://doi.org/10.1016/j.compeleceng.2018.01.011

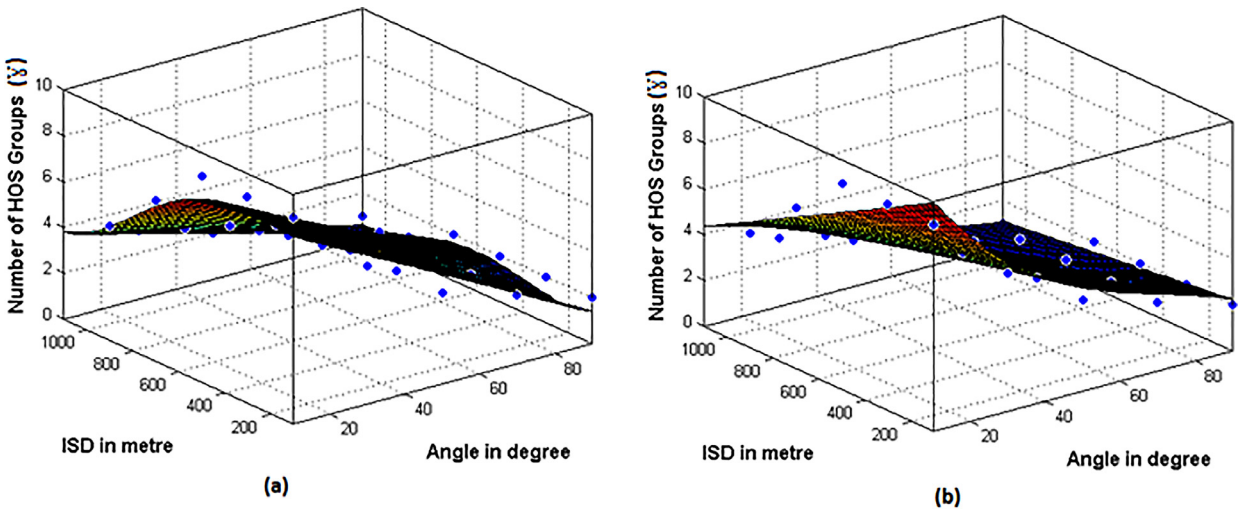

Fig. 11. Surface polynomial model for a) p = 1, q = 4 and b) p = 4, q = 1.

4.6. Model formulation

The above dependency identified from the analysis has been modeled, to resemble the behavior of a regression model. Based on this model, it is possible to accurately identify the combinations of HCP values that can be configured when information about α and β_{ISD} is known. To measure the prediction accuracy of the model, goodness-of-fit metrics are measured, based on SSE, R-squared, adjusted R-squared and RMSE. The SSE metric measures the deviation between the predicted and the simulated data. Values closer to zero indicate the coincidence of the predicted data with the simulated data. The R-squared metric presents the level of correlation between the predicted and simulated response values. It indicates the proportion of variance accounted for by the model. Similarly, an adjusted R-squared statistic with a value close to 1 indicates a better fit, while a value of RMSE close to 0 indicates that the deviation between the predicted and simulated values is lower, and the model is more useful for prediction. Hence, the model which results in a better "goodness of fit" is finalized as the model with higher accuracy of prediction. Different orders with respect to the dependent factors were studied, as the order of the model controls the accuracy. Two cases with the same and different degrees are modeled and discussed below.

4.6.1. Case 1: polynomial with different degree

The polynomial obtained for p = 1 and q = 4 is presented in Eq. (14). The values of coefficients within 95% confidence limits are $\varphi_1 = 9.002$, $\phi_2 = -0.07499$, $\phi_3 = -0.00121$, $\phi_4 = -0.0001194$, $\phi_5 = 1.674e{-}05$, $\phi_6 = 2.902e{-}07$, $\phi_7 = -4.074e{-}08$, $\phi_8 = -1.389e{-}10$ and$\phi_9 = 2.083e{-}11$. The goodness-of-fit metrics for the developed polynomial are SSE = 6.746, R-squared = 0.9565, adjusted R-squared = 0.9399 and RMSE = 0.5668.

$$\gamma = f(\alpha, \beta_{ISD}) = \varphi_1 + \varphi_2\alpha + \varphi_3\beta_{ISD} + \varphi_4\alpha\beta_{ISD} + \varphi_5\beta_{ISD}^2 + \varphi_6\alpha\beta_{ISD}^2 + \varphi_7\beta_{ISD}^3 + \varphi_8\alpha\beta_{ISD}^3 + \varphi_9\beta_{ISD}^4 \quad (14)$$

Eq. (15) represents the polynomial for p = 4 and q = 1. The coefficient values of the polynomial are $\phi_1 = 13.18$, $\phi_2 = -0.2942$, $\phi_3 = -0.007784$, $\phi_4 = 0.003019$, $\phi_5 = 0.0002537$, $\phi_6 = -8.135e{-}06$, $\phi_7 = -3.744e{-}06$, $\phi_8 = -4.34e{-}08$ and $\phi_9 = 1.935e{-}08$.

$$\gamma = f(\alpha, \beta_{ISD}) = \varphi_1 + \varphi_2\alpha + \varphi_3\beta_{ISD} + \varphi_4\alpha^2 + \varphi_5\alpha\beta_{ISD} + \varphi_6\alpha^3 + \varphi_7\alpha^2\beta_{ISD} + \varphi_8\alpha^4 + \varphi_9\alpha^3\beta_{ISD} \quad (15)$$

The goodness-of-fit metrics for the developed polynomial are SSE = 6.827, R-squared = 0.9559, adjusted R-squared = 0.9392 and RMSE = 0.5702.

Fig. 11 represents the surface polynomial model obtained for the degrees (p = 1 and q = 4) and (p = 4 and q = 1). It is inferred that the fitness of the model with the simulated value has more deviation for the lower degree predictor, such as p = 1 in Fig. 11(a) and q = 1 in Fig. 11(b).

4.6.2. Case 2: polynomial with same degree

The polynomial when p = q = 1 is presented in Eq. (16). The values of coefficients within 95% confidence limits are $\phi_1 = 8.97$, $\phi_2 = -0.0675$ and $\phi_3 = -0.002714$. The goodness-of-fit metrics for the developed polynomial are SSE = 19.83, R-squared = 0.872, adjusted R-squared = 0.8626 and RMSE = 0.857.

$$\gamma = f(\alpha, \beta_{ISD}) = \varphi_1 + \varphi_2\alpha + \varphi_3\beta_{ISD} \quad (16)$$

Eq. (17) represents the polynomial when p = q = 4. The coefficients of the polynomial are $\phi_1 = 11.75$, $\phi_2 = -0.2752$, $\phi_3 = -0.004069$, $\phi_4 = 0.003058$, $\phi_5 = 0.0001027$, $\phi_6 = 1.701e{-}05$, $\phi_7 = -8.135e{-}06$, $\phi_8 = -3.935e{-}06$, $\phi_9 = 2.742e{-}07$,

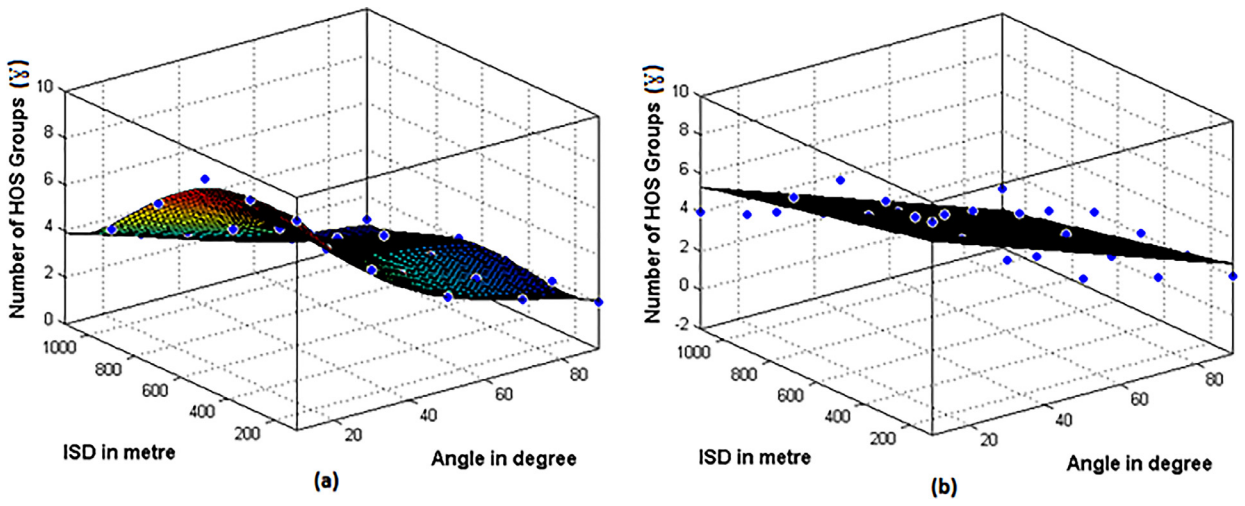

Fig. 12. Surface polynomial model for a) p = q = 4 and b) p = q = 1.

Table 5
Regression models with their performance metrics.

Polynomial (Poly'pq')	SSE	R-square	Adjusted R-square	RMSE
Poly55 (p = 5 & q = 5)	0.4773	0.9969	0.9901	0.2303
Poly44 (p = 4 & q = 4)	0.94	0.9939	0.9883	0.2503
Poly33 (p = 3 & q = 3)	1.964	0.9873	0.9816	0.3134
Poly22 (p = 2 & q = 2)	3.722	0.976	0.971	0.3938
Poly11 (p = 1 & q = 1)	19.83	0.872	0.8626	0.857
Poly15 (p = 1 & q = 5)	6.729	0.9566	0.9337	0.5951
Poly14 (p = 1 & q = 4)	6.746	0.9565	0.9399	0.5668
Poly13 (p = 1 & q = 3)	7.523	0.9515	0.9388	0.5719
Poly12 (p = 1 & q = 2)	8.02	0.9482	0.94	0.5664
Poly51 (p = 5 & q = 1)	9.027	0.9417	0.9111	0.6893
Poly41 (p = 4 & q = 1)	6.827	0.9559	0.9392	0.5702
Poly31 (p = 3 & q = 1)	7.071	0.9544	0.9425	0.5545
Poly21 (p = 2 & q = 1)	8.332	0.9462	0.9376	0.5773

$\phi_{10} = -4.074e{-}08$, $\phi_{11} = -4.34e{-}08$, $\phi_{12} = 1.935e{-}08$, $\phi_{13} = 1.594e{-}10$, $\phi_{14} = -1.389e{-}10$ and $\phi_{15} = 2.083e{-}11$. The goodness-of-fit metrics for the developed fourth-degree polynomial are SSE = 0.94, R-squared = 0.9939, adjusted R-squared = 0.9883 and RMSE = 0.2503.

$$\gamma = f(\alpha, \beta_{ISD}) = \varphi_1 + \varphi_2\alpha + \varphi_3\beta_{ISD} + \varphi_4\alpha^2 + \varphi_5\alpha\beta_{ISD} + \varphi_6\beta_{ISD}^2 + \varphi_7\alpha^3 + \varphi_8\alpha^2\beta_{ISD} + \varphi_9\alpha\beta_{ISD}^2 + \varphi_{10}\beta_{ISD}^3 + \varphi_{11}\alpha^4 + \varphi_{12}\alpha^3\beta_{ISD} + \varphi_{13}\alpha^2\beta_{ISD}^2 + \varphi_{14}\alpha\beta_{ISD}^3 + \varphi_{15}\beta_{ISD}^4 \quad (17)$$

Fig. 12 represents the obtained surface polynomial for the above models. The coincidence of the simulated data with the model prediction is observed for the higher degree. The conclusion from the results presented for polynomials of the same and different degree, is that the higher the degree of the polynomial the better the goodness of fit, and vice-versa. The goodness-of-fit values for the different possible combinations of polynomial degree were computed as shown in Table 5. As previously mentioned, an increase in the goodness of fit is observed with increases in the degree of the model. However, the amount of computation increases for a higher-degree polynomial because (N + 1) terms are added to a polynomial of degree N.

From Table 5, it can be seen that the Poly55 model has the smallest value of SSE. However, a marginal difference exists between the models Poly55 and Poly44, compared to the other models. Similarly, a lower deviation is observed for the other metrics such as adjusted R-squared and RMSE. For example, the Poly44 model has an R-squared value of 0.9939, while the Poly55 model has an R-squared value of 0.9969. This indicates that the Poly44 model has a prediction accuracy of 99.39%, while the Poly55 model has an accuracy of 99.69%. The difference in prediction accuracy between Poly44 and Poly55 is marginal. This clearly indicates that the achievement of 0.30% improvement in accuracy by Poly55 requires an addition of seven terms to the model compared to Poly44. Therefore, in this study, the polynomial model Poly44 is adopted as the proposed RBP model.

Please cite this article as: S.P. A, B. P.T.V, Regression model for handover control parameter configuration in LTE-A networks, Computers and Electrical Engineering (2018), https://doi.org/10.1016/j.compeleceng.2018.01.011

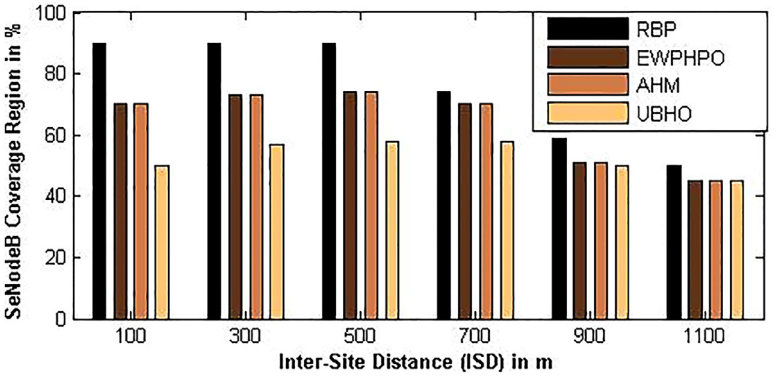

Fig. 13. Serving eNodeB coverage region for different β_{ISD}.

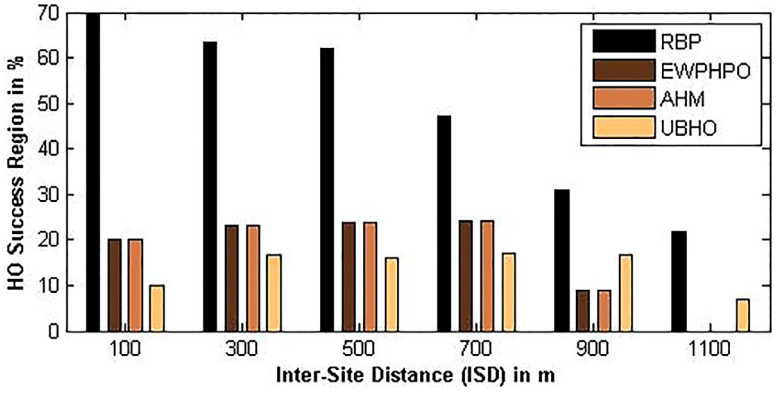

Fig. 14. HO success region for different β_{ISD}.

4.7. Performance metrics analysis

A comparison of the developed RBP model with the existing methods in enhanced weighted performance based HO parameter optimization (EWPHPO) [9], adaptive hysteresis margin (AHM) [12] and user behavior based optimization (UBHO) [15] is presented, as mentioned in Section 2. This is performed via two performance metrics, namely, the serving eNodeB coverage region (R_{SeNBC}) and the HO success region (R_{HOS}). The metric R_{SeNBC} refers to the region within which the UE can be offered service by the serving eNodeB, (i.e., before HO) and also the region where HO to the target eNodeB can be achieved successfully. The metric R_{HOS} defines the region between the serving and target eNodeB in which an HO, initiated at any point results in success. The scenario considered for comparison is the urban environment and macro-macro deployment with varying β_{ISD} and an α of 50°.

Fig. 13 presents the comparison of the existing methods EWPHPO, AHM and UBHO with the developed RBP in terms of R_{SeNBC}. The inference is that the developed RBP method achieves a larger serving eNodeB coverage region for all values of β_{ISD}. Furthermore, methods EWPHPO and AHM produce similar results, as the impact of TTT is assumed to be negligible for high mobility UE. The existing AHM method produces better results for low mobility UE, compared to the EWPHPO method. The conclusion drawn is that the developed RBP model, when compared to EWPHPO and AHM, achieves an average 28.6% increase in R_{SeNBC} up to 500 m of β_{ISD}, with a 57.14% improvement with respect to UBHO. When β_{ISD} is increased beyond 500 m, the improvement of the developed model is 10.46% compared with the first two methods and 18.6% compared with the latter method.

A similar comparison is made on the basis of R_{HOS}. The result obtained is presented in Fig. 14. As previously mentioned, the response of the EWPHPO and AHM methods is the same, due to the negligible impact of the TTT value. The developed RBP model achieves an average 184.63% increase in performance, compared to EWPHPO and AHM and an average 285.4% improvement with respect to UBHO. Despite a reduction in the HOS region as β_{ISD} increases, the developed model outperforms the existing methods. A larger HOS region implies that the network operator has more flexibility in selecting the HCP, and there is a higher probability of HOS. In addition, the provision of more flexibility in turn requires an efficient optimization approach to further define the optimal setting, as mentioned in the UBHO method. Hence, the practical realization of the presented work demands the implementation of efficient machine learning techniques. This is planned as future research.

Please cite this article as: S.P. A, B. P.T.V, Regression model for handover control parameter configuration in LTE-A networks, Computers and Electrical Engineering (2018), https://doi.org/10.1016/j.compeleceng.2018.01.011

5. Conclusion and future work

Initially, the significance of considering all the control parameters in improving the HO performance was studied. Consideration of all the parameters in HCP configuration improved the HO performance in terms of the success rate. A sensitivity analysis was performed, to study the impact of control parameters on the region of HOS with respect to β_{ISD}. The analysis was extended to the UE characteristics of (α). High dependency of HO performance was observed with respect to β_{ISD} and α. Hence, a regression model was developed utilizing β_{ISD} and α. The order of the model was varied, and the resulting variations studied with a view to improving the prediction accuracy. The developed models were validated for goodness of fit, and the Poly44 model was found to demonstrate a prediction accuracy of 99.39% compared to the other models. Hence, this study was confined to the RBP (Poly44) model.

Finally, the presented RBP method was compared with three other methods, namely, EWPHPO, AHM and UBHO in terms of R_{SeNBC} and R_{HOS}. The ability of the presented model to provide improved performance in terms of both metrics was observed, and also the presented method doesn't rely on expert knowledge in framing rules. Fluctuation in the HO performance does not occur, as the presented method depends on the network and UE based distance related metrics. Hence, the developed RBP model plays an important role in improving the HO performance, compared with a fixed HCP configuration. In future work, a reinforcement learning-based mechanism should be adopted for choosing the optimal setting from the reduced set of parameters, and for meeting the requirements of the network operator as well as dealing with the dynamic nature of the wireless network. This work could be extended to the HetNet environment involving small cells for improving overall network performance.

Supplementary materials

Supplementary material associated with this article can be found, in the online version, at doi:10.1016/j.compeleceng.2018.01.011.

References

[1] Kottkamp M, Roessler A, Schlienz J, LTE-advanced technology introduction, White paper - Rohde & Schwarz, 1MA169_3E-August 2012.
[2] Parkvall S, Furuskar A, Dahlman E. Evolution of LTE toward IMT-advanced. IEEE Commun Mag 2011;49(February(2)). https://doi.org/10.1109/MCOM.2011.5706315.
[3] Contains I, Hedlund A. HetNets: opportunities and challenges, White paper. An Ascom Network Testing; 2013.
[4] A comprehensive tutorial on the LTE Network Architecture, Alcatel-Lucent; 2009. White paper.
[5] 3GPP, Universal Mobile Telecommunications System (UMTS); LTE; Non-Access-Stratum (NAS) protocol for Evolved Packet System (EPS), (Release 13) (March 2016). TS 24.301, V13.4.0, 3rd Generation Partnership Project (3GPP).
[6] 3GPP, LTE; Telecommunication Management; Performance Management (PM); Performance measurements Evolved Universal Terrestrial Radio Access Network (E-UTRAN), (Release 13) (March 2016). TS 32.425, V13.3.0, 3rd Generation Partnership Project (3GPP).
[7] 3GPP, LTE; General Packet Radio Service (GPRS) enhancements for Evolved Universal Terrestrial Radio Access Network (E-UTRAN), (Release 13) (March 2016). TS 23.401, V13.5.0, 3rd Generation Partnership Project (3GPP).
[8] 3GPP, Evolved Universal Terrestrial Radio Access (E-UTRA); Radio Resource Control (RRC); Protocol specification, (Release 13) (April 2016). TS 36.331, V13.1.0, 3rd Generation Partnership Project (3GPP).
[9] Mihaela Balan I, Sas B, Jansen T, Moerman I, Spaey K, Demeester P. An enhanced weighted performance-based handover parameter optimization algorithm for LTE networks. EURASIP J Wireless Commun Netw 2011:1–11. http://dx.doi.org/10.1186/1687-1499-2011-98.
[10] Munoz P, Barco R, de la Bandera I. On the potential of handover parameter optimization for self-organizing networks. IEEE Trans Veh Technol 2013:1895–905. http://dx.doi.org/10.1109/TVT.2013.2247778.
[11] Fatty BKS, Lin P-C. Mobility robustness optimization in wireless mobile networks. In: Seventh international conference on ubiquitous and future networks (ICUFN), July; 2015. p. 624–9. https://doi.org/10.1109/icufn.2015.7182619.
[12] Becvar Z, Mach P. Adaptive hysteresis margin for handover in femtocell networks. In: Sixth international conference on wireless and mobile communications. IEEE Computer Society; 2010. p. 256–61. http://dx.doi.org/10.1109/icwmc.2010.17.
[13] Lee D-W, Gil G-T, Kim D-H. A cost-based adaptive handover hysteresis scheme to minimize the handover failure rate in 3GPP LTE system. EURASIP J Wireless Commun Netw 2010:1–7. https://doi.org/10.1155/2010/750173.
[14] Zheng W, Zhang H, Chu X, Wen X. Mobility robustness optimization in self: organizing LTE Femtocell networks. EURASIP J Wireless Commun Netw 2013:1–10. http://dx.doi.org/10.1186/1687-1499-2013-27.
[15] Hegazy RD, Nasr OA. A user behavior based handover optimization algorithm for LTE networks. In: IEEE wireless communications and networking conference (WCNC); 2015. p. 1255–60. http://dx.doi.org/10.1109/wcnc.2015.7127649.
[16] Lim J, Hong D. Mobility and handover management for heterogeneous networks in LTE-advanced. J Wireless Pers Commun 2013:2901–12. Springer https://doi.org/10.1007/s11277-013-1187-8.
[17] Mehta M, Akhtar N, Karandikar A. Impact of handover parameters on mobility performance in LTE HetNets. In: Twenty-first national conference on communications (NCC); 2015. p. 1–6. http://dx.doi.org/10.1109/ncc.2015.7084910.
[18] Kollias G, Adelantado F, Verikoukis C. The impact of inter-site distance and time-to-trigger on handover performance in LTE-A HetNets. In: IEEE - international conference on communications (ICC), June; 2015. p. 3969–74. http://dx.doi.org/10.1109/icc.2015.7248944.
[19] Saraswathi Priyadharshini A, Bhuvaneswari PTV. A study on HO parameter optimization in LTE-A networks. In: IEEE-international conference on microelectronics, computing and communications (MicroCom); January; 2016. p. 1–5. http://dx.doi.org/10.1109/MicroCom.2016.7522429
[20] http://web.maths.unsw.edu.au/~adelle/Garvan/Assays/GoodnessOfFit.html.
[21] 3GPP, Technical Specification Group Radio Access Network; Evolved Universal Terrestrial Radio Access (E-UTRA); Mobility enhancements in heterogeneous networks, (Release 11) (December 2012). TR 36.839, V11.1.0 (2012-12), 3rd Generation Partnership Project (3GPP).
[22] 3GPP, Technical Specification Group Radio Access Network; Evolved Universal Terrestrial Radio Access (E-UTRA); Further advancements for E-UTRA physical layer aspects, (Release 9) (March 2010). TR 36.814, V9.0.0, 3rd Generation Partnership Project (3GPP).

Please cite this article as: S.P. A, B. P.T.V, Regression model for handover control parameter configuration in LTE-A networks, Computers and Electrical Engineering (2018), https://doi.org/10.1016/j.compeleceng.2018.01.011

A. Saraswathi Priyadharshini received the B.Tech. degree of Information Technology in 2010, and the M.E. in Embedded System Technologies in 2013. Currently, working towards the Ph.D. degree with the Department of Electronics Engineering, MIT Campus, Anna University, Chennai, India. Her research areas include communication systems (LTE), Wireless Sensor Networks, Embedded Systems and Operating Systems.

P.T.V. Bhuvaneswari received her Ph.D. degree from Anna University. She is working as Assistant Professor (Senior Grade) in the Department of Electronics Engineering, MIT Campus, Anna University. She has successfully completed five sponsored research projects. She has authored about fifty four national and international conferences and nine international journals. Her research focus includes Wireless Communication, Networking, IoT, and Computer Networks.

Please cite this article as: S.P. A, B. P.T.V, Regression model for handover control parameter configuration in LTE-A networks, Computers and Electrical Engineering (2018), https://doi.org/10.1016/j.compeleceng.2018.01.011